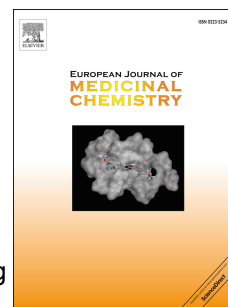# Accepted Manuscript

Development of novel amino-quinoline-5,8-dione derivatives as NAD(P)H:quinone oxidoreductase 1 (NQO1) inhibitors with potent antiproliferative activities

Yong Ling, Qiu-Xing Yang, Yu-Ning Teng, Shi Chen, Wei-Jie Gao, Jing Guo, Pei-Ling Hsu, Yue Liu, Susan L. Morris-Natschke, Chin-Chuan Hung, Kuo-Hsiung Lee

Please cite this article as: Y. Ling, Q.-X. Yang, Y.-N. Teng, S. Chen, W.-J. Gao, J. Guo, P.-L. Hsu, Y. Liu, S.L. Morris-Natschke, C.-C. Hung, K.-H. Lee, Development of novel amino-quinoline-5,8-dione derivatives as NAD(P)H:quinone oxidoreductase 1 (NQO1) inhibitors with potent antiproliferative activities, *European Journal of Medicinal Chemistry* (2018), doi: 10.1016/j.ejmech.2018.05.025.

Development of novel amino-quinoline-5,8-dione derivatives as NAD(P)H:quinone oxidoreductase 1 (NQO1) inhibitors with potent antiproliferative activities

Yong Ling[a,b,1], Qiu-Xing Yang[a,1], Yu-Ning Teng[b,c], Shi Chen[a], Wei-Jie Gao[a], Jing Guo[a], Pei-Ling Hsu[b], Yue Liu[a], Susan L. Morris-Natschke[b], Chin-Chuan Hung[c,*], Kuo-Hsiung Lee[b,d*]

[a]School of Pharmacy and Jiangsu Province Key Laboratory for Inflammation and Molecular Drug Target, Nantong University, Nantong 226001, PR China.
[b]Natural Products Research Laboratories, UNC Eshelman School of Pharmacy, University of North Carolina, Chapel Hill, North Carolina 27599, United States
[c]Department of Pharmacy, College of Pharmacy, China Medical University, Taichung 40402, Taiwan
[d]Chinese Medicine Research and Development Center, China Medical University and Hospital, Taichung 40402, Taiwan

Abstract: Fourteen novel amino-quinoline-5,8-dione derivatives (**6a-h** and **7a-h**) were designed and synthesized by coupling different alkyl- or aryl-amino fragments at the C6- or C7-position of quinoline-5,8-dione. All target compounds showed antiproliferative potency in the low micromolar range in both drug sensitive HeLaS3 and multidrug resistant KB-vin cell lines. Compounds **6h**, **6d**, **7a**, and **7d** exhibited more potent antiproliferative effects than the other compounds. Especially, compounds **6d** and **7d** displayed NQO1-dependent cytotoxicity and competitive NQO1 inhibitory effects in both drug sensitive HeLaS3 and multidrug resistant KB-vin cell lines. Furthermore, compounds **6h**, **6d**, **7a**, and **7d** induced a dose-dependent lethal mitochondrial dysfunction in both drug sensitive HeLaS3 and multidrug resistant KB-vin cells by increasing intracellular reactive oxygen species (ROS) levels. Notably, compound **7d** selectively inhibited cancer cells, but not non-tumor liver cell proliferation *in vitro*, and significantly triggered HeLaS3 cell apoptosis by regulating apoptotic proteins of Bcl-2, Bax, and cleaved caspase-3 in a dose-dependent manner. Our findings suggest that these novel C6- or C7-substituted amino-quinoline-5,8-dione derivatives, such as **7d**, could be further developed in the future as potent and selective antitumor agents to potentially circumvent multi-drug resistance (MDR).

[1]These authors contributed equally to this work.
*Corresponding author.
E-mail addresses: khlee@unc.edu (K.H. Lee), cc0206hung@gmail.com (C.C. Hung).

1. Introduction

Due to aberrant metabolic events and abnormal proliferative growth phenotypes, reactive oxygen species (ROS) levels are commonly elevated in cancer cells [1-3]. To cope with an increase in intrinsic oxidative stress, cancer cells augment their antioxidant capacity through upregulation of antioxidant enzymes [4]. In doing so, cancer cells become more dependent on the elevated antioxidant capacity for growth and survival, which makes them susceptible when oxidative stress is further elevated through production of more ROS and/or inhibition of elevated antioxidant enzymes [4,5]. Therefore, a feasible strategy in cancer chemotherapy is to selectively target cancer cells based on the different redox states between normal and tumor cells [1,6-8], particularly when such targeting involves a redox adaptive mechanism that confers drug resistance [2].

In this context, inhibition of NAD(P)H:quinone oxidoreductase 1 (NQO1) has emerged as a promising redox-modulating strategy for anticancer therapy. NQO1 is a ubiquitous flavoenzyme that catalyzes the two-electron reduction of quinones to hydroquinones. It is intimately involved with cancer and upregulated in several human tumor cells, such as pancreas, colon, breast, lung, liver, stomach, kidney, and ovaries, at levels of up to 50-fold greater than in normal tissue [9,10]. Moreover, NQO1 is found in the cytosol, Golgi complex, nucleus, mitochondria, cellular membrane, and endoplasmic reticulum, as well as extracellularly [11–14]. The NQO1 and glutathione systems are the two major cellular thiol antioxidant systems that can be targeted for anticancer therapy [15-18]. Many human cancers can reportedly be killed selectively through rapid ROS generation mediated by NQO1 bioreduction (Fig. 1).
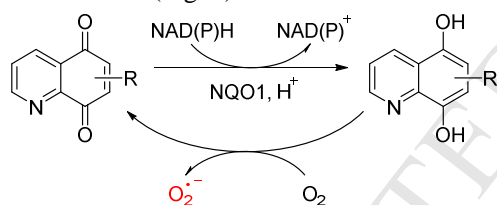

Fig. 1. NQO1-mediated redox cycling of quinolinediones.

Recent findings suggest that some quinolinediones are excellent substrates of NQO1 and are selectively cytotoxic to cancer cell lines that overexpress NQO1, but not to normal cell lines [17–23]. These findings form the basis for the development of novel quinoline-5,8-dione derivatives as potential NQO1-directed cytotoxicity agents, which efficiently regulate the intracellular human NQO1 dependent redox cycling and thus the ROS generated in the progress (Fig. 1). Moreover, small substituents such as amine groups at the C-6 or C-7 positions of the quinoline-5,8-dione moiety favorably impacted binding to the active site of NQO1 [16,17,24,25]. In this study, we coupled different alkyl- or aryl-amino fragments to the C6- or C7-position of quinoline-5,8-dione to design novel amino-quinoline-5,8-dione derivatives, and compared the cytotoxic effects of these compounds. In addition, because most quinolinedione derivatives usually have poor water solubility, we introduced hydrophilic groups at the end of arylamino fragments to improve the lipid-aqueous partition coefficient. Herein, we report our synthesis of novel amino-quinoline-5,8-dione derivatives (**6a–6h** and **7a–7h**, Table 1), as well as evaluation of their cytotoxicity effects and mechanisms in multiple

cancer cell lines.

2. Results and discussion

2.1 Chemistry
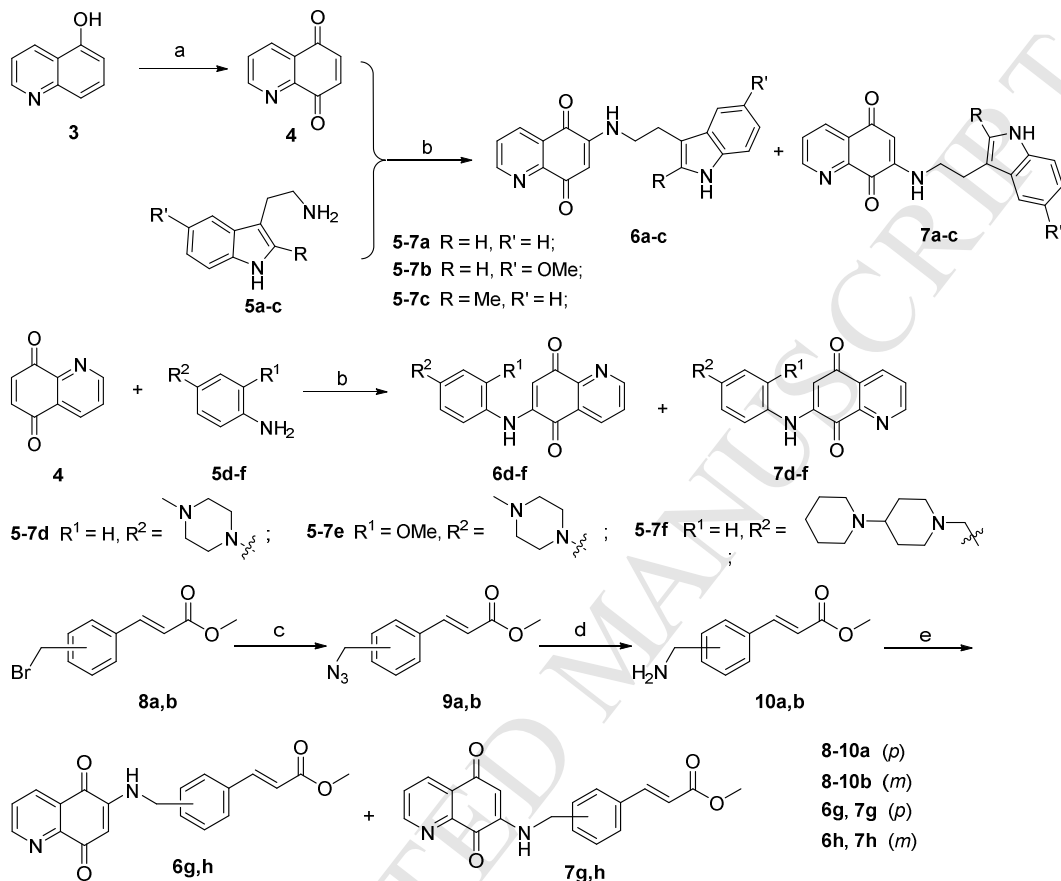
Scheme 1. Reagents and conditions: (a) iodobenzene diacetate, $CH_3CN:H_2O$ = 2:1, 0 □, 2h, 86%; (b) MeOH, rt, 6 h, 31-43%; (c) NaN_3, DMF, rt, 2 h; (d) PPh_3, anhydrous THF, rt, 2 h; (e) quinolinedione **4**, MeOH, rt, 6 h, 22-41%.

Scheme 1 summarizes the syntheses of the quinolinedione derivatives **6a–6h** and **7a–7h**. Quinoline-5,8-dione (**4**) was prepared from 5-hydroxyquinoline (**3**) by oxidation with iodobenzene diacetate (PIDA) in a mixture of $CH_3CN:H_2O$ (2:1) according to Barret's method [26]. Compound **4** was subsequently treated with different substituted 2-(1*H*-indol-3-yl)ethanamines (**5a–5c**) or anilines (**5d–5f**) in MeOH to obtain the target compounds **6a–6c** and **7a–7c** or **6d–6f** and **7d–7f**, respectively. This is a non-regioselective Michael addition to give the hydroquinone followed by an autoxidation back to quinone. Often, only catalytic base and air are needed for such oxidations [27]. Fortunately, these two regioisomers were easy separated by column chromatography ($CH_2Cl_2/MeOH$= 20/1), and the major isomers were **6a–6f**. In addition, treatment of (*E*)-methyl 3-(4-(bromomethyl)phenyl) acrylate **8a** or (*E*)-methyl 3-(3-(bromomethyl)phenyl) acrylate **8b** in DMF with NaN_3 produced intermediate **9a,b**. Then intermediate **9a,b** was treated with PPh_3 in THF to furnish compounds **10a,b**, which were further reacted with quinoline-5,8-dione **4** in the presence of MeOH to produce target

compound **6g, 7g** or **6h, 7h**. All target compounds were purified by column chromatography, and their structures were confirmed by ^1H NMR, ^{13}C NMR, MS, and HRMS. Each target compound was >95% pure as determined by high-performance liquid chromatography and could be used for subsequent experiments.

2.2 Antiproliferative activity against both sensitive and resistant human cervical cancer cells

To evaluate the antiproliferative activity of the target compounds, we initially tested their effects on the proliferation of parental sensitive cervical epithelioid carcinoma cells HeLaS3 and multi-drug resistant human cervical cancer cells KB-vin (both cell lines are used to investigate the cytotoxicity effect and antidrug resistance of potential drugs *in vitro*) by the SRB assay using paclitaxel as a positive control. The IC_{50} values of individual compounds against each tumor cell line are presented in Table 1. The results showed that all target compounds displayed antiproliferative potency in the low micromolar range against both drug sensitive HeLaS3 and multidrug resistant KB-vin cell lines. Some compounds, such as **6h**, **6d**, **7a**, and **7d**, exhibited significant antiproliferative effects with IC_{50} values between 0.80 and 1.52 μM. These four compounds displayed comparable or greater potency than paclitaxel (IC_{50} = 1.01 μM) against multidrug resistant KB-vin cells. Structurally, the addition of a 4-(4-methylpiperazin-1-yl)phenylamino group to position-6 (**6d**) or -7 (**7d**) of quinoline-5,8-dione led to the greatest antiproliferative potency against both HeLaS3 (IC_{50} 0.80 and 0.59 μM, respectively) and KB-vin (IC_{50} 1.52 and 0.97 μM, respectively) cell lines. Compounds **6h** (6-amino-(3-methylphenyl)acrylic ester) and **7a** (7-aminoethylindole) showed comparable potency to **7d** against KB-vin, but not HeLasS3, cells. Indeed, all other compounds were significantly less potent (IC_{50} 3.40–6.24 μM) against the two tested cancer cell lines, even those with only slight structural differences (e.g., **6e** and **7e** have a 2-methoxy group in addition to the 4-(4-methylpiperazin-1-yl) group found on the phenylamino side chain of **6d** and **7d**).

Table 1. *In vitro* antiproliferative data of **6a-h** and **7a-h** against HeLaS3 and KB-vin cells.

Compounds	$IC_{50}{}^a$ (μM)		Compounds	IC_{50} (μM)	
	HeLaS3^b	KB-vin^c		HeLaS3	KB-vin
6a	6.24 ± 1.12	5.12 ± 0.23	**7a**	4.53 ± 0.35	1.10 ± 0.12
6b	5.50 ± 0.61	6.20 ± 0.08	**7b**	6.12 ± 0.33	4.00 ± 0.39
6c	6.64 ± 0.04	4.92 ± 0.62	**7c**	6.21 ± 0.08	5.98 ± 0.58
6d	0.80 ± 0.02	1.52 ± 0.04	**7d**	0.59 ± 0.03	0.97 ± 0.01
6e	5.26 ± 0.34	4.03 ± 0.26	**7e**	4.37 ± 0.36	4.69 ± 0.29
6f	5.16 ± 0.22	5.23 ± 0.36	**7f**	5.07 ± 0.10	6.19 ± 0.59
6g	5.84 ± 0.49	3.40 ± 0.35	**7g**	5.67 ± 0.62	5.62 ± 0.26
6h	5.36 ± 0.22	0.91 ± 0.03	**7h**	4.99 ± 0.16	4.27 ± 0.29
			Paclitaxel	0.013 ± 0.0014	1.01 ± 0.11

^{a} The inhibitory effects of individual compounds on the proliferation of cancer cell lines were determined by the SRB assay. The data are expressed as the mean ± SD of three independent experiments data.

^{b} Human cervical epithelioid carcinoma cell line.

^{c} Multi-drug resistant human cervical cancer cell line
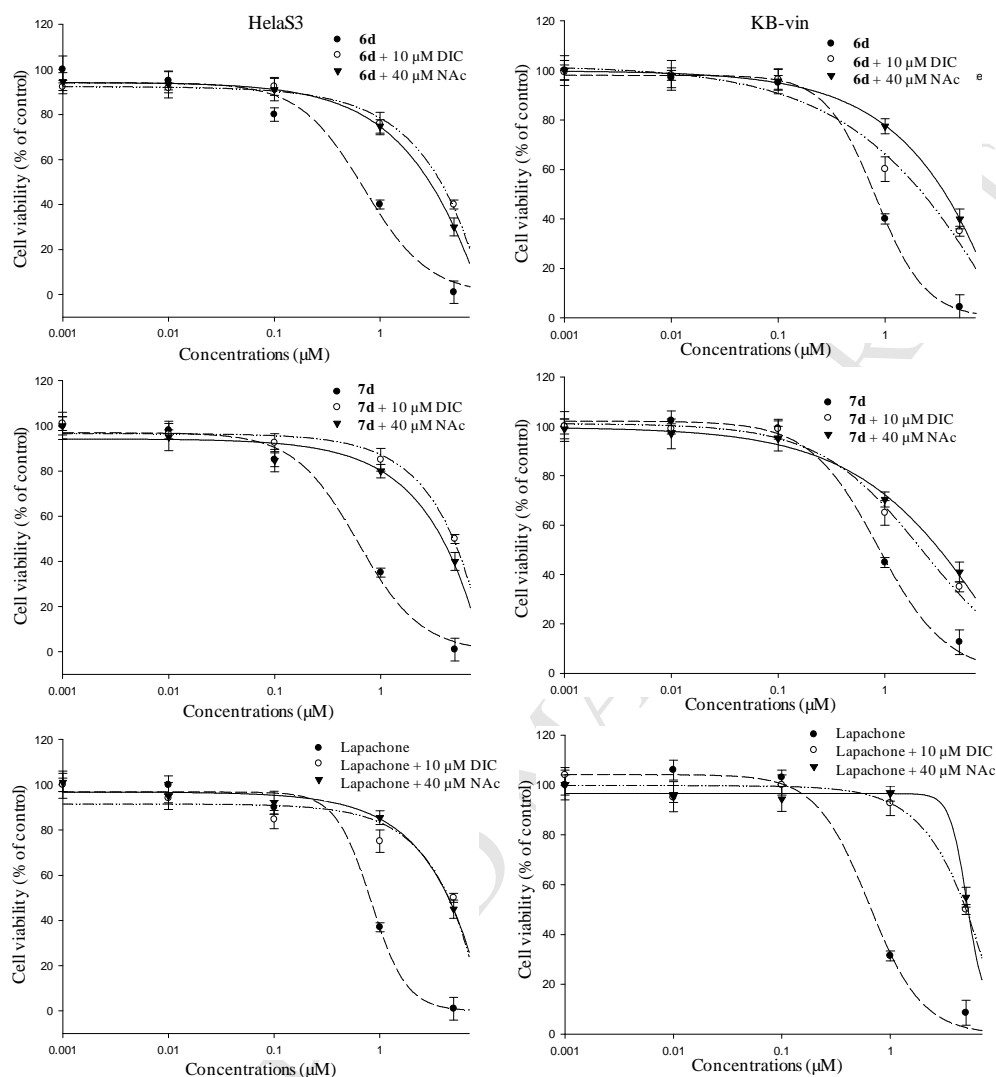
2.3 NQO1-dependency assessments

Fig. 2. Evaluations of NQO1-dependent cytotoxicity of testing compounds. The cell viability was evaluated by combination treatment of 10 μM DIC or 40 μM NAc with testing compounds, using SRB assay after 72 h treatment.

Within the drug concentration range tested, the compounds **6d** and **7d** showed the most potent cytotoxicities against both drug sensitive HeLaS3 and multidrug resistant KB-vin cell lines. To deepen our knowledge about the mechanism of action of compounds **6d** and **7d**, we examined their potential NQO1-dependent cytotoxicities, with or without dicoumarol (DIC, an NQO1 inhibitor) and *N*-acetylcysteine (NAc, a free radical scavenger). Based on the survival curves (Fig. 2), the cell viabilities of compound-treated HeLaS3 and KB-vin cells were significantly increased by the addition of DIC and NAc. The cytotoxic IC_{50} values were greater than 3 μM against both cell lines in the presence of **6** or **7**, DIC, and NAc, but much lower in the presence of compound alone (**6d** only: 0.8

μM, HeLaS3 and 1.52 μM, KB-vin; **7d** only: 0.59 μM HeLaS3 and 0.97 μM, KB-vin). These results suggested that the cytotoxic effects of **6d** and **7d** were NQO1-specific in both drug sensitive HeLaS3 and multidrug resistant KB-vin cell lines.
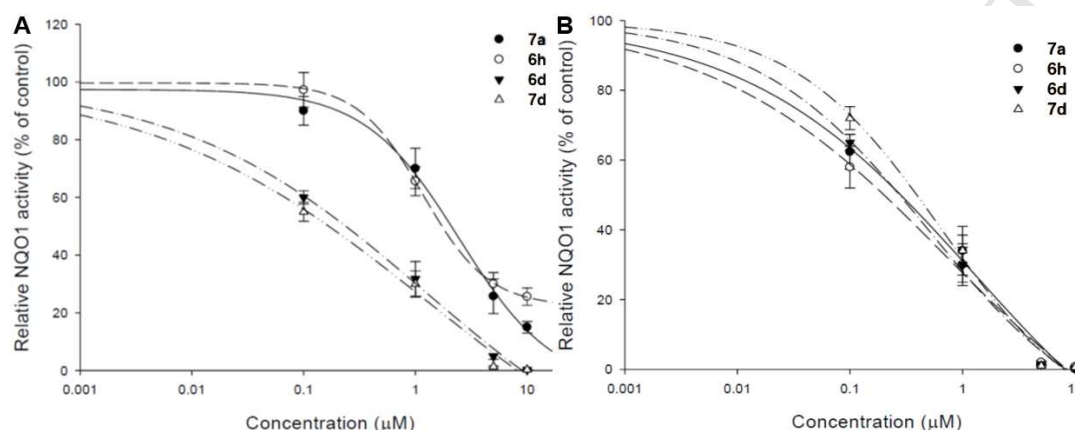
2.4 NQO1 inhibitory activities and kinetics

Fig. 3. NQO1 activity of (a) HeLa cells (b) KB-vin cells after compound treatment. The HeLa and KB-vin cells were treated with serial concentrations of **6h**, **6d**, **7a**, and **7d** for 24 h. NQO1 activity was detected by the NQO1 activity assay kit (catalog number: ab184867), and was significantly altered after treatment with **6h**, **6d**, **7a**, and **7d** for 24 h.

Table 2. Effects of **6h**, **6d**, **7a**, and **7d** on NQO1 activity in HeLaS3 (parental) and KB-vin (MDR) cancer cell lines.

Compound	IC$_{50}$ (μM)					
	HeLaS3			KB-vin		
7a	6.25	±	1.25	0.55	±	0.01
6h	5.25	±	0.90	0.53	±	0.05
6d	0.47	±	0.07	0.56	±	0.01
7d	0.44	±	0.08	0.57	±	0.02

Based on the encouraging antiproliferative activity of **6a-h** and **7a-h** against HeLaS3 and KB-vin cells, we further tested a selected group of compounds (**6h**, **6d**, **7a**, and **7d**) for *in vitro* inhibitory activity against NQO1. As shown in Fig. 3, the NQO1 activities in both drug sensitive HeLaS3 and multidrug resistant KB-vin cell lines were inhibited dose-dependently after 24 h treatment with **6h**, **6d**, **7a**, and **7d**. Particularly, compounds **6d** and **7d** were more potent NQO1 inhibitors than **6h** and **7a** in drug sensitive HeLaS3 cells. On the other hand, **6h**, **6d**, **7a**, and **7d** showed similar NQO1 inhibitory effects in multidrug resistant KB-vin cells (Table 2). Therefore, these four compounds displayed dose-dependent NQO1 inhibitory activity.
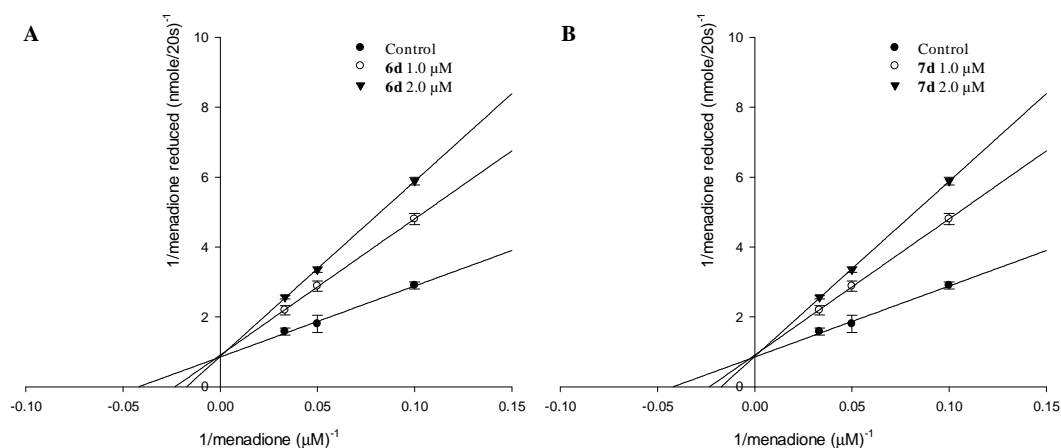
Fig. 4. Enzyme kinetics for compound **6d** and **7d** using recombinant human NQO1. Lineweaver-Burk plot for NQO1 inhibition demonstrated that **6d** and **7d** competitively inhibited NQO1 activity.

The NQO1 inhibitory kinetics of **6d** and **7d** indicated competitive inhibition as demonstrated by the Lineweaver-Burk plots (Fig. 4). As the concentration of **6d** increased, the maximum rate (V_{max}) remained the same (12.5±1.2 nmol/mg protein/20s) and the affinity (K_m) increased (no treatment control: 30.22 ± 2.5 μM; addition of 1.0 μM **6d**: 45.27 ± 5.33 μM; addition of 2.0 μM **6d**: 60.15 ± 3.51 μM). In terms of **7d**, as the concentration of **7d** increased, the maximum rate (V_{max}) remained the same (11.03±1.5 nmole/mg protein/20s) and the affinity (K_m) increased (no treatment control: 20.30 ± 0.97 μM; addition of 1.0 μM **7d**: 40.17 ± 2.31 μM; addition of 2.0 μM **7d**: 55.17 ± 1.49 μM). These results indicated that **6d** and **7d** are competitive inhibitors of NQO1.

2.5 Treatment with quinolinedione derivatives increases ROS levels

We next examined whether the killing effect of quinolinedione derivatives on cervical cancer cells involved increasing ROS levels. ROS levels in both drug sensitive HeLaS3 and multidrug resistant KB-vin cell lines were assessed by flow cytometry using the redox-sensitive fluorescent probe 2′,7′-dichlorofluorescein diacetate (DCFH-DA). As shown in Fig. 5, the ROS production increased dose-dependently in both drug sensitive HeLaS3 and multidrug resistant KB-vin cell lines after 24 h treatment with **6h**, **6d**, **7a**, and **7d**. These findings suggested that treatment with **6h**, **6d**, **7a**, and **7d** lead to increased oxidative stress in both drug sensitive HeLaS3 and multidrug resistant KB-vin cell lines, which causes significant cytotoxicity in tumor cells.
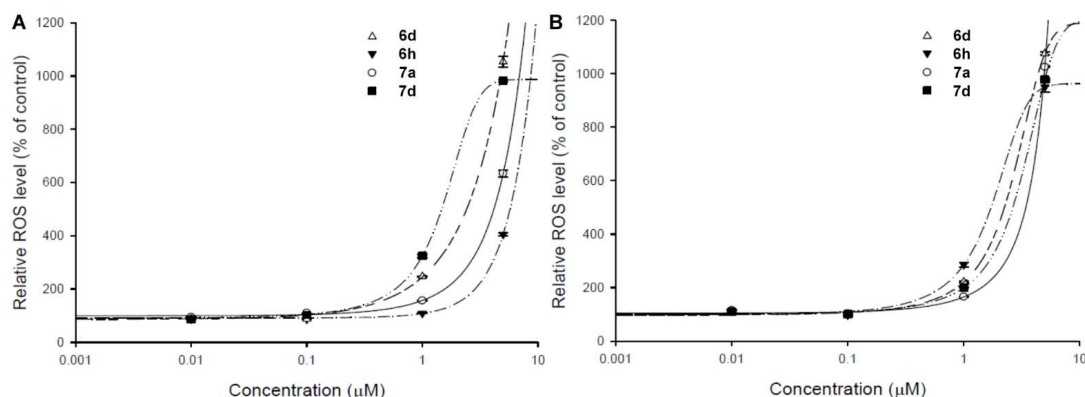
Fig. 5. Reactive oxygen species (ROS) generation of (a) HeLa cells (b) KB-vin cells after compound treatment. The HeLa and KB-vin cells were treated with serial concentrations of PL, **6h**, **6d**, **7a**, and **7d** for 24 h. The generated ROS were detected by the ROS-Glo^{TM} H_2O_2 assay kit (catalog number: G8821), and increased significantly after treatment with **6h**, **6d**, **7a**, and **7d** for 24 h.

2.4 Quinolinedione derivatives induce mitochondrial dysfunction

It is well known that mitochondria are central to the regulation of apoptosis. Loss of mitochondrial membrane potential ($\triangle\psi$m) is catastrophic for cells and leads to the release of cytochrome C into the cytosol [28]. The mitochondrial membrane potential of both drug sensitive HeLaS3 and multidrug resistant KB-vin cell lines were significantly decreased in a dose-dependent manner after 24 h treatment with **6h**, **6d**, **7a**, and **7d** (Fig. 6).
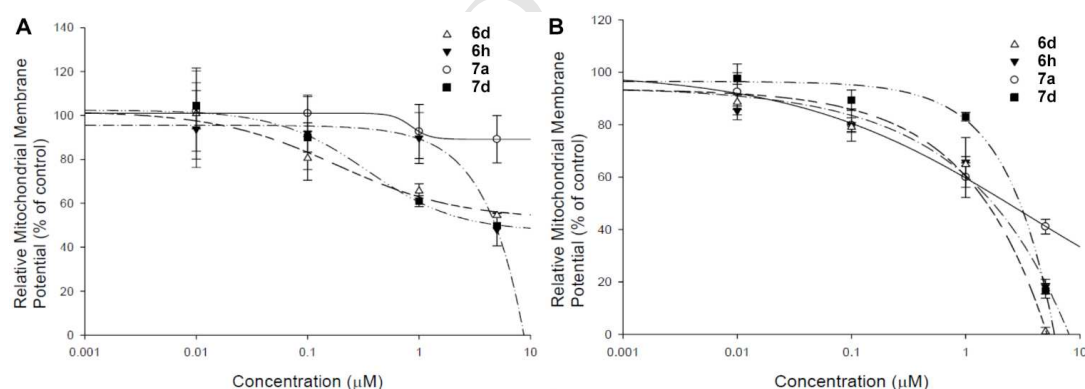
Fig. 6. Changes of mitochondrial membrane potential (MMP) in (a) HeLa cells (b) KB-vin cells after compound treatment. The HeLa and KB-vin cells were treated with serial concentrations of PL, **6h**, **6d**, **7a**, and **7d** for 24 h. The MMP was detected by the MITO-ID® membrane potential cytotoxicity kit (catalog number: ENZ-51019-KP002), and decreased significantly after treatment with **6h**, **6d**, **7a**, and **7d** for 24 h in drug-resistant KB-vin cells.

2.5 The selectivity of quinolinedione derivatives to tumor cells

Given the strong antiproliferative and NQO1 inhibitory effects of **7d** *in vitro*, we investigated the selectivity profile by examining inhibitory effects on the growth of both cancer HeLaS3 cells and normal endometrial epithelial cells (EECs). Treatment with increasing doses of **7d** had no significant

effect on the survival of non-tumor EECs, while the same treatment regimen induced major HeLaS3 cell death (Fig. 7), suggesting that **7d** might possess selective antiproliferative activity against tumor cells.
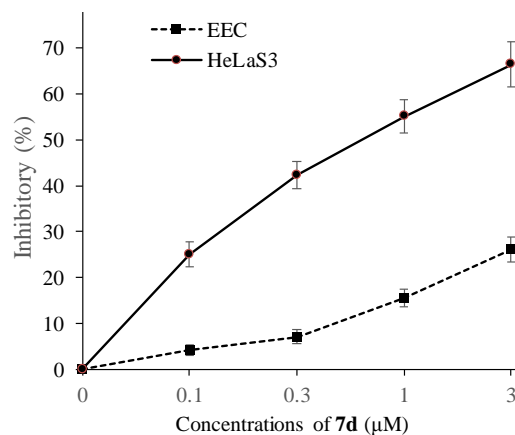

Fig. 7. Inhibitory effects of **7d** on the proliferation of HeLaS3 and EEC cells. Cells were incubated with the indicated concentrations of **7d** for 72 h. Cell proliferation was assessed using the MTT assay. Data are expressed as means ± SD of the inhibition (%) from three independent experiments.

2.6 Quinolinedione derivatives induce apoptosis in HeLaS3 cells.

To determine whether the inhibitory effects of **7d** on cervical carcinoma cell proliferation are accompanied by enhanced cancer cell apoptosis, HeLaS3 cells were incubated with different concentrtions of **7d** for 72 h, and the percentages of apoptotic cells were determined by FITC-Annexin V/PI double staining and flow cytometry. As shown in Fig. 8, the percentage of annexin V + apoptotic HeLaS3 cells gradually increased for those cells exposed to increasing concentrations of **7d** (12.8% for 0.2 μM; 27.6% for 0.6 μM; and 66.3% for 1.8 μM), demonstrating that incubation with **7d** induced HeLaS3 cell apoptosis in a dose-dependent manner.
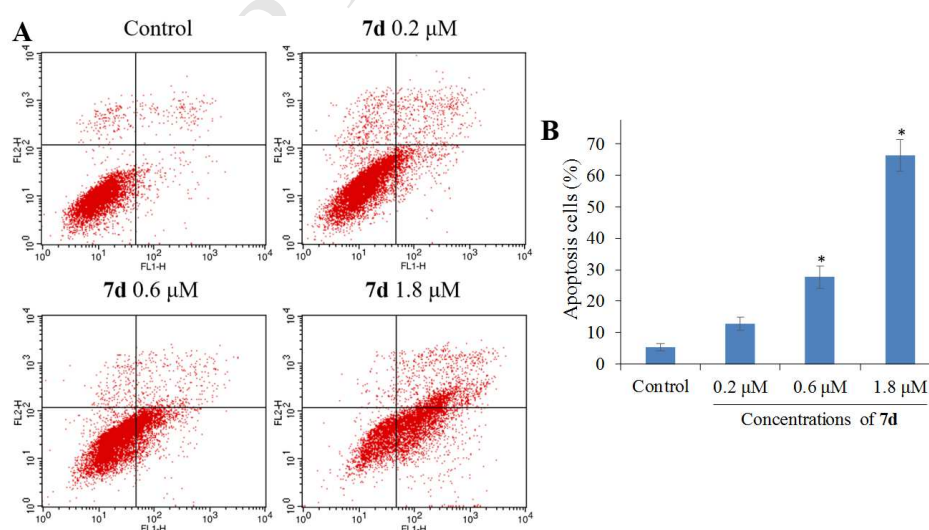
Fig. 8. Compound **7d** induces HeLaS3 cell apoptosis *in vitro*. HeLaS3 cells were incubated with the indicated concentrations of **7d** for 72 h, and the cells were stained with FITC-Annexin V/PI, followed by flow cytometry analysis. (A) Flow cytometry analysis. (B) Quantitative analysis of apoptotic cells. Data are expressed as means ± SD of the percentages of apoptotic cells from three independent experiments. *$P < 0.01$ vs control.
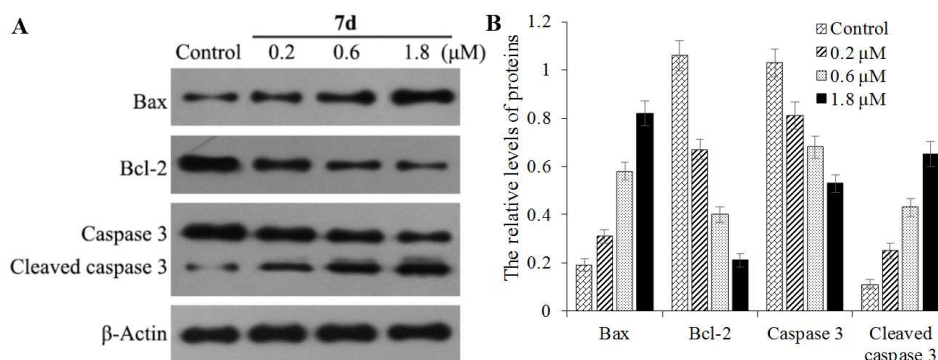

Fig. 9. (A) The expression of Bax, Bcl-2, Caspase 3, and β-actin was examined by western blot analysis. HeLaS3 cells were incubated with or without **7d** at the indicated concentrations for 72 h and the levels of protein expression were detected using specific antibodies. Data shown are representative images of each protein for three separate experiments. (B) Quantitative analysis of Bax, Bcl-2, and Caspase 3. The relative levels of each protein compared to control β-actin were determined by densimetric scanning. Data are expressed as means ± SD from three separate experiments. *$P < 0.01$ vs respective control.

To further investigate the induction of apoptosis by **7d**, we examined the expression of apoptotic proteins Bax, Bcl-2, and the cleavage states of caspase-3, in response to **7d** treatment (Fig. 9). Sub-confluent HeLaS3 cervical carcinoma cells were treated with or without **7d** for 72 h, and then lysed and analyzed by western blot. β-Actin expression was used as an internal control. The treatment with **7d** dramatically increased the relative levels of pro-apoptotic Bax expression but reduced the levels of anti-apoptotic Bcl-2 expression in a dose-dependent manner. Furthermore, compound **7d** treatment also induced more cleavage of caspase-3 than the control group (Fig. 8A and 8B). Taken together, these results confirm that **7d** treatment induced apoptosis in HeLaS3 cells.

3. Conclusion

In summary, we have designed and synthesized novel amino-quinoline-5,8-dione derivatives **6a-h** and **7a-h** by coupling different alkyl- or aryl-amino fragments at the C6- or C7-position of quinoline-5,8-dione, and then evaluated their biological activities in various *in vitro* assays. All target compounds showed antiproliferative potency in the low micromolar range in both drug sensitive HeLaS3 and multidrug resistant KB-vin cell lines. Among them, compounds **6d** and **7d** exhibited NQO1-dependent antiproliferative effects with IC$_{50}$ values between 0.59 and 1.52 μM, as well as competitive NQO1 inhibitory effects in both drug sensitive HeLaS3 and multidrug resistant KB-vin cell lines. Furthermore, compounds **6h**, **6d**, **7a**, and **7d** induced a dose-dependent lethal mitochondrial dysfunction in both drug sensitive HeLaS3 and multidrug resistant KB-vin cells by increasing intracellular ROS levels. Notably, compound **7d** selectively inhibited cancer cells but not non-tumor liver cell proliferation *in vitro*, and significantly induced HeLaS3 cell apoptosis by reducing the

anti-apoptotic protein levels of Bcl-2 and up-regulating the pro-apoptotic proteins of Bax and cleaved caspase-3 in a concentration dependent manner. Taken together, these results suggest that these novel C6- or C7-substituted amino-quinoline-5,8-dione derivatives, such as **7d**, could be further developed as potent and selective antitumor agents to potentially circumvent MDR.

4. Experimental section

The synthesized compounds were purified by column chromatography using silica gel (300–400 mesh) except for recrystallization and thin-layer chromatography (TLC) using silica gel 60 F_{254} plates (250 mm; Qingdao Ocean Chemical Company, China). ^{1}H NMR and ^{13}C NMR spectra were recorded with a Bruker Avance 400 MHz spectrometer at 300 K, using TMS as an internal standard. MS spectra were recorded on a Mariner Mass Spectrum (ESI). High resolution mass spectra were recorded with a hybrid LTQ FT (ICR 7T) (ThermoFisher, Bremen, Germany) mass spectrometer coupled with a Waters Acquity H-class liquid chromatograph system. All solvents were reagent grade and, when necessary, were purified and dried by standard methods. Solutions after reactions and extractions were concentrated using a rotary evaporator operating at a reduced pressure of ca. 20 Torr. Organic solutions were dried over anhydrous sodium sulfate.

4.1. General procedure for synthesis of quinoline-5,8-dione (4)

A solution of iodobenzene diacetate (10.35 mmol, 3.3 g) in 12 mL CH_3CN:H_2O (2:1) was added to quinolin-5-ol (**3**) (3.45 mmol, 0.50 g) at 0 □ under N_2 and stirred for 1h. After the reaction was completed, water (40 mL) was added, and the solution was extracted with EtOAc (3 × 20 mL). The organic phase was washed by brine and concentrated in vacuo to give **4** as a yellow solid, yield 82%. MS (ESI) m/z = 160 [M+H]$^+$.

4.2. General procedure for synthesis of 10a, b

4.2.1. (E)-Methyl 3-(4-(aminomethyl)phenyl)acrylate (10a)

To a solution of (*E*)-methyl 3-(4-(bromomethyl)phenyl)acrylate **8a** (0.1 g, 0.39 mmol) in 4 mL DMF, NaN_3 (38.2 mg, 0.59 mmol) was added and the mixture was stirred at rt for 2 h. After the reaction was completed, 20 mL water were added and the solution was extracted with EtOAc (3 × 20 mL). The organic phase was washed by brine, dried over anhydrous sodium sulfate, and evaporated in vacuo to give **9a**, which was then dissolved in 3 mL THF. Triphenylphosphine was added and the mixture was stirred at rt for 2h. Then, 1 mL water was added and the mixture was stirred for 1 h. The solution was extracted with EtOAc (3 × 5 mL). The organic phase was combined and washed with brine, dried over anhydrous sodium sulfate, and evaporated in vacuo. The residue was purified by column chromatography (EA/PE = 2/1) on silica gel to afford **10a** as a clear translucent oil in 52% yield. MS (ESI) m/z = 192 [M+H]$^+$.

4.2.1. (E)-Methyl 3-(3-(aminomethyl)phenyl)acrylate (10b)

Compound **10b** was synthesized from (*E*)-methyl 3-(3-(bromomethyl)phenyl)acrylate **8b**, according to the synthetic procedure for **10a** in a yield of 52%. MS (ESI) m/z = 192 [M+H]$^+$.

4.3. General procedure for synthesis of 6a, 7a

Quinoline-5,8-dione (**4**) (149.1 mg, 0.94 mmol) was added to a solution of 2-(1H-indol-3-yl)ethanamine (**5a**) (100.0 mg, 0.63 mmol) in MeOH (4 mL) at rt. The mixture was stirred at rt for 16 h and evaporated *in vacuo*. The residue was purified by column chromatography (CH₂Cl₂/MeOH= 20/1) to give **6a** and **7a** in yields of 40% and 26%, respectively.

4.3.1. 6-((2-(1H-Indol-3-yl)ethyl)amino)quinoline-5,8-dione (6a)

Analytical data for **6a**: ^{1}H NMR (d_6-DMSO, 400 MHz): δ 10.87 (s, 1H, NH), 8.91 (m, 1H, Ar-H), 8.31 (m, 1H, Ar-H), 7.82 (m, 2H, NH, Ar-H), 7.78 (d, 1H, J = 8.0 Hz, Ar-H), 7.36 (m, 2H, Ar-H), 7.28 (m, 2H, Ar-H), 5.80 (s, 1H, CH), 3.53 (m, 2H, CH₂), 3.06 (m, 2H, CH₂). ^{13}C NMR (d_6-DMSO, 100 MHz): δ 180.8, 180.2, 153.0, 149.4, 147.1, 136.7, 133.9, 130.7, 128.9, 127.5, 123.6, 123.5, 121.5, 118.6, 111.9, 111.6, 99.1, 43.2, 23.7. MS (ESI) m/z =318 [M+H]$^+$; MS (ESI) m/z = 318 [M+H]$^+$; HRMS (ESI): m/z calcd for C₁₉H₁₆N₃O₂: 318.1243; found: 318.1231 [M+H]$^+$.

4.3.2. 7-((2-(1H-Indol-3-yl)ethyl)amino)quinoline-5,8-dione (7a)

Analytical data for **7a**: ^{1}H NMR (d_6-CD₃OD, 400 MHz): δ 8.83 (m, 1H, NH), 8.42 (m, 1H, Ar-H), 7.79 (dd, 1H, J = 4.0 Hz, J = 4.0 Hz, Ar-H), 7.60 (s, 1H, Ar-H), 7.31 (m, 2H, NH, Ar-H), 6.99-7.15 (m, 4H, Ar-H), 5.78 (s, 1H, CH), 3.51 (m, 2H, CH₂), 3.04 (m, 2H, CH₂). ^{13}C NMR (d_6-DMSO, 100 MHz): δ 180.8, 180.2, 153.1, 149.4, 147.1, 136.7, 133.9, 130.8, 129.1, 127.6, 123.6, 123.5, 121.4, 118.6, 111.9, 111.6, 99.2, 43.1, 24.0. MS (ESI) m/z =318 [M+H]$^+$; MS (ESI) m/z = 318 [M+H]$^+$; HRMS (ESI): m/z calcd for C₁₉H₁₆N₃O₂: 318.1243; found: 318.1241 [M+H]$^+$.

4.4. General procedure for synthesis of 6b, 7b

Compounds **6b** and **7b** were synthesized from quinoline-5,8-dione (**4**), 2-(5-methoxy-1H-indol-3-yl)ethanamine (**5b**), according to the synthetic procedure for compounds **6a** and **7a** in yields of 41% and 23%, respectively.

4.4.1. 6-((2-(5-Methoxy-1H-indol-3-yl)ethyl)amino)quinoline-5,8-dione (6b)[29]

Analytical data for **6b**: ^{1}H NMR (d_6-DMSO, 400 MHz): δ 10.71(s, 1H, NH), 8.96 (m, 1H, Ar-H), 8.32 (d, 1H, J = 4.0 Hz, Ar-H), 7.72 (m, 2H, Ar-H, NH), 7.22 (m, 2H, Ar-H), 7.06 (d, 1H, J = 4.0 Hz, Ar-H), 6.71 (m, 1H, Ar-H), 5.87 (s, 1H, CH), 3.76 (s, 3H, OCH₃), 3.48 (m, 2H, CH₂), 3.00 (m, 2H, CH₂). ^{13}C NMR (d_6-DMSO, 100 MHz): δ 182.0, 180.3, 155.0, 153.5, 149.2, 148.4, 134.3, 131.8, 128.0, 127.9, 127.9, 126.9, 124.2, 112.5, 111.6, 111.4, 101.1, 100.4, 55.8, 43.1, 23.8. MS (ESI) m/z = 348 [M+H]$^+$; HRMS (ESI): m/z calcd for C₂₀H₁₈N₃O₃: 348.1348; found: 348.1344 [M+H]$^+$.

4.4.2. 7-((2-(5-Methoxy-1H-indol-3-yl)ethyl)amino)quinoline-5,8-dione (7b)

Analytical data for **7b**: ^{1}H NMR (d_6-CD₃OD, 400 MHz): δ 8.79 (m, 1H, Ar-H), 8.36 (d, 1H, J = 4.0 Hz, Ar-H), 7.76 (m, 1H, Ar-H), 7.18 (m, 3H, J = 6.0 Hz, NH, Ar-H), 6.70 (m, 1H, Ar-H), 5.75 (s, 1H, CH), 3.75 (s, 3H, OCH₃), 3.45 (m, 2H, CH₂), 3.08 (m, 2H, CH₂). ^{13}C NMR (d_6-DMSO, 100 MHz): δ 182.0, 180.3, 155.0, 153.5, 149.3, 148.4, 134.3, 131.8, 128.0, 127.9, 126.9, 124.2, 112.5, 111.6, 111.4,

101.1, 100.4, 55.7, 41.1, 23.8. MS (ESI) m/z = 348 [M+H]$^+$; HRMS (ESI): m/z calcd for $C_{20}H_{18}N_3O_3$: 348.1348; found: 348.1343 [M+H]$^+$.

4.5. General procedure for synthesis of 6c, 7c

Compounds **6c** and **7c** were synthesized from quinoline-5,8-dione (**4**), 2-(2-methyl-1H-indol-3-yl) ethanamine (**5c**), according to the synthetic procedure for compounds **6a** and **7a** in yields of 38% and 25%, respectively.

4.5.1. 6-((2-(2-Methyl-1H-indol-3-yl)ethyl)amino)quinoline-5,8-dione (6c)

Analytical data for **6c**: ^{1}H NMR (d_6-DMSO, 400 MHz): δ 10.78 (s, 1H, NH), 8.96 (d, 1H, J = 4.0 Hz, Ar-H), 8.33 (d, 1H, J = 8.0 Hz, Ar-H), 7.73 (m, 3H, NH, Ar-H), 7.24 (d, 1H, J = 8.0 Hz, Ar-H), 7.00 (m, 2H, Ar-H), 5.80 (s, 1H, CH), 3.39 (m, 2H, CH$_2$), 2.98 (m, 2H, CH$_2$), 2.34 (s, 3H, CH$_3$). ^{13}C NMR (d_6-DMSO, 100 MHz): δ 182.0, 180.3, 155.0, 149.2, 135.6, 134.4, 134.2, 132.8, 128.6, 127.8, 126.9, 117.6, 117.5, 110.9, 107.2, 101.0, 43.1, 22.8, 11.7. MS (ESI) m/z = 332 [M+H]$^+$; HRMS (ESI): m/z calcd for $C_{20}H_{18}N_3O_2$: 332.1399; found: 332.1390 [M+H]$^+$.

4.5.2. 7-((2-(2-Methyl-1H-indol-3-yl)ethyl)amino)quinoline-5,8-dione (7c)

Analytical data for **7c**: ^{1}H NMR (d_6-DMSO, 400 MHz): δ 10.78 (s, 1H, NH), 8.90 (d, 1H, J = 4.0 Hz, Ar-H), 8.31 (d, 1H, J = 8.0 Hz, Ar-H), 7.81 (m, 1H, Ar-H), 7.78 (m, 1H, Ar-H), 7.48 (d, 1H, J = 8.0 Hz, Ar-H), 7.24 (d, 1H, J = 8.0 Hz, Ar-H), 6.98 (m, 2H, Ar-H), 5.74 (s, 1H, CH), 3.41 (m, 2H, CH$_2$), 2.98 (m, 2H, CH$_2$), 2.34 (s, 3H, CH$_3$). ^{13}C NMR (d_6-DMSO, 100 MHz): δ 180.7, 180.2, 153.0, 149.3, 147.0, 135.6, 134.0, 132.8, 130.7, 129.0, 128.9, 128.6, 117.7, 117.6, 110.9, 107.3, 99.0, 43.2, 22.8, 11.6. MS (ESI) m/z = 332 [M+H]$^+$; HRMS (ESI): m/z calcd for $C_{20}H_{18}N_3O_2$: 332.1399; found: 332.1389 [M+H]$^+$.

4.6. General procedure for synthesis of 6d, 7d

Compounds **6d** and **7d** were synthesized from quinoline-5,8-dione (**4**), 4-(4-methyl piperazin-1-yl)aniline (**5d**), according to the synthetic procedure for compounds **6a** and **7a** in yields of 39% and 24%, respectively.

4.6.1. 6-((4-(4-Methylpiperazin-1-yl)phenyl)amino)quinoline-5,8-dione (6d)

Analytical data for **6d**: ^{1}H NMR (d_6-DMSO, 400 MHz): δ 9.14 (s, 1H, NH), 8.94 (d, 1H, J = 4.0 Hz, Ar-H), 8.36 (d, 1H, J = 8.0 Hz, Ar-H), 7.72 (m, 1H, Ar-H), 7.19 (d, 2H, J = 8.0 Hz, Ar-H), 6.97 (d, 2H, J =8.0 Hz, Ar-H), 6.09 (s, 1H, CH), 3.13 (m, 4H, CH$_2$), 2.52 (m, 4H, CH$_2$), 2.18 (s, 3H, CH$_3$). ^{13}C NMR (d_6-DMSO, 100 MHz): δ 182.1, 181.1, 154.9, 149.1, 148.8, 146.6, 134.4, 129.0, 128.0, 127.0, 125.2, 116.0, 102.4, 54.9, 48.3, 46.1. MS (ESI) m/z = 349 [M+H]$^+$; HRMS (ESI): m/z calcd for $C_{20}H_{21}N_4O_2$: 349.1665; found: 349.1660 [M+H]$^+$.

4.6.2. 7-((4-(4-Methylpiperazin-1-yl)phenyl)amino)quinoline-5,8-dione (7d)

Analytical data for **7d**: ^{1}H NMR (d_6-DMSO, 400 MHz): δ 9.30 (s, 1H, NH), 8.94 (s, 1H, Ar-H), 8.31(s, 1H, J = 8.0 Hz, Ar-H), 7.82 (s, 1H, Ar-H), 7.23 (d, 2H, J = 8.0 Hz, Ar-H), 7.02 (d, 2H, J = 8.0

Hz, Ar-H), 5.99 (s, 1H, CH), 3.16 (m, 4H, CH$_2$), 2.40 (m, 4H, CH$_2$), 2.26 (m, 3H, CH$_3$). ^{13}C NMR (d_6-DMSO, 100 MHz): δ 181.6, 180.3, 153.1, 149.2, 147.7, 147.1, 133.7, 130.3, 129.1, 128.9, 125.3, 116.0, 100.5, 54.9, 48.3, 46.1. MS (ESI) m/z = 349 [M+H]$^+$; HRMS (ESI): m/z calcd for C$_{20}$H$_{21}$N$_4$O$_2$: 349.1665; found: 349.1658 [M+H]$^+$.

4.7. General procedure for synthesis of 6e, 7e

Compounds **6e** and **7e** were synthesized from quinoline-5,8-dione (**4**), 2-methoxy-4-(4-methylpiperazin-1-yl)aniline (**5e**), according to the synthetic procedure for compounds **6a** and **7a** in yields of 36% and 22%, respectively.

4.7.1. 6-((2-Methoxy-4-(4-methylpiperazin-1-yl)phenyl)amino)quinoline-5,8-dione (6e)

Analytical data for **6e**: ^{1}H NMR (d_6-CD$_3$OD, 400 MHz): δ 8.89 (d, 1H, J = 4.0 Hz, Ar-H), 8.48 (d, 1H, J = 8.0 Hz, Ar-H), 7.73 (m, 1H, Ar-H), 7.23 (d, 1H, J = 8.0 Hz, Ar-H), 6.68 (s, 1H, Ar-H), 6.62 (d, 1H, J = 8.0 Hz, Ar-H), 6.04 (s, 1H, CH), 4.53 (m, 4H, CH$_2$), 3.88 (s, 3H, OCH$_3$), 3.28 (m, 4H, CH$_2$), 2.35 (s, 3H, NCH$_3$). ^{13}C NMR (d_6-DMSO, 100 MHz): δ 182.0, 181.6, 155.0, 148.6, 147.9, 146.3, 141.9, 135.9, 130.3, 130.1, 128.1, 125.2, 124.0, 113.9, 103.4, 56.5, 55.1, 48.3, 46.1. MS (ESI) m/z = 379 [M+H]$^+$; HRMS (ESI): m/z calcd for C$_{21}$H$_{23}$N$_4$O$_3$: 379.1770; found: 379.1759 [M+H]$^+$.

4.7.2. 7-((2-Methoxy-4-(4-methylpiperazin-1-yl)phenyl)amino)quinoline-5,8-dione (7e)

Analytical data for **7e**: ^{1}H NMR (d_6-CD$_3$OD, 400 MHz): δ 8.85 (d, 1H, J = 4.0 Hz, Ar-H), 8.42 (m, 1H, Ar-H), 7.80 (m, 1H, Ar-H), 7.22 (d, 1H, J = 8.0 Hz, Ar-H), 6.68 (m, 2H, Ar-H), 5.94 (s, 1H, CH), 4.62 (m, 4H, CH$_2$), 3.85 (s, 3H, OCH$_3$), 2.61 (m, 4H, CH$_3$), 2.34 (s, 3H, NCH$_3$). ^{13}C NMR (d_6-DMSO, 100 MHz): δ 182.0, 181.7, 155.1, 155.0, 148.6, 146.3, 142.3, 134.7, 130.5, 130.0, 128.1, 127.4, 124.0, 114.9, 103.5, 56.8, 55.3, 49.6, 46.2. MS (ESI) m/z = 379 [M+H]$^+$; HRMS (ESI): m/z calcd for C$_{21}$H$_{23}$N$_4$O$_3$: 379.1770; found: 379.1767 [M+H]$^+$.

4.8. General procedure for synthesis of 6f, 7f

Compounds **6f** and **7f** were synthesized from quinoline-5,8-dione (**4**), 4-([1,4'-bipiperidin]-1'-ylmethyl)aniline (**5f**), according to the synthetic procedure for compounds **6a** and **7a** in yields of 38% and 23%, respectively.

4.8.1. 6-((4-([1,4'-Bipiperidin]-1'-yl)phenyl)amino)quinoline-5,8-dione (6f)

Analytical data for **6f**: ^{1}H NMR (d_6-DMSO, 400 MHz): δ 9.30 (s, 1H, NH), 9.00 (m, 1H, Ar-H), 8.43 (m, 1H, Ar-H), 7.80 (m, 1H, Ar-H), 7.37 (m, 2H, Ar-H), 6.72 (d, 2H, J = 8.0 Hz, Ar-H), 6.20 (s, 1H, CH), 3.44 (s, 2H, CH$_2$), 2.51 (m, 8H, CH$_2$), 2.19 (s, 1H, CH), 1.94 (m, 2H, CH$_2$), 1.68 (m, 2H, CH$_2$), 1.47 (m, 6H, CH$_2$). ^{13}C NMR (d_6-DMSO, 100 MHz): δ 182.1, 181.5, 155.0, 154.8, 148.7, 146.5, 135.2, 134.5, 132.8, 130.2, 128.1, 127.2, 124.2, 103.2, 62.5, 57.1, 53.0, 51.3, 29.4, 24.9, 22.5. MS (ESI) m/z = 431 [M+H]$^+$; HRMS (ESI): m/z calcd for C$_{26}$H$_{31}$N$_4$O$_2$: 431.2447; found: 431.2433 [M+H]$^+$.

4.8.2. 7-((4-([1,4'-Bipiperidin]-1'-yl)phenyl)amino)quinoline-5,8-dione (7f)

Analytical data for **6f**: ^{1}H NMR (d_6-DMSO, 400 MHz): δ 9.37 (s, 1H, NH), 8.96 (m, 1H, Ar-H), 8.32 (m, 1H, Ar-H), 7.85 (d, 1H, J = 4.0 Hz, Ar-H), 7.42 (m, 2H, Ar-H), 6.46 (d, 2H, J = 8.0 Hz, Ar-H), 6.07 (s, 1H, CH), 3.46 (s, 2H, CH$_2$), 2.50 (s, 8H, CH$_2$), 2.19 (m, 1H, CH), 1.89 (m, 2H, CH$_2$), 1.67 (m, 2H, CH$_2$), 1.43 (m, 6H, CH$_2$). ^{13}C NMR (d_6-DMSO, 300 MHz): δ 182.1, 174.9, 153.3, 147.6, 147.2, 135.7, 135.3, 133.8, 130.2, 128.9, 124.2, 101.4, 61.1, 55.9, 53.3, 49.9, 29.4, 24.9, 22.5. MS (ESI) m/z = 431 [M+H]$^+$; HRMS (ESI): m/z calcd for C$_{26}$H$_{31}$N$_4$O$_2$: 431.2447; found: 431.2433 [M+H]$^+$.

4.9. General procedure for synthesis of 6g, 7g

Compounds **6g** and **7g** were synthesized from quinoline-5,8-dione (**4**), (*E*)-methyl 3-(4-(aminomethyl)phenyl)acrylate (**10a**), according to the synthetic procedure for compounds **6a** and **7a** in yields of 40% and 23%, respectively.

4.9.1. (E)-Methyl 3-(4-(((5,8-dioxo-5,8-dihydroquinolin-6-yl)amino)methyl)phenyl)acrylate (6g)

Analytical data for **6g**: ^{1}H NMR (d_6-CD$_3$OD, 400 MHz): δ 8.87 (m, 1H, Ar-H), 8.43 (m, 1H, Ar-H), 7.59-7.71 (m, 4H, Ar-H), 7.40 (m, 2H, Ar-H), 6.51 (d, 1H, J = 16.0 Hz, CH), 5.77 (s, 1H, CH), 4.52 (s, 2H, CH$_2$), 3.74 (s, 3H, OCH$_3$). ^{13}C NMR (d_6-DMSO, 100 MHz): δ 181.9, 180.6, 167.0, 154.9, 149.0, 148.6, 144.8, 138.6, 134.6, 129.6, 128.1, 127.6, 127.5, 126.9, 118.6, 102.1, 52.0, 45.2. MS (ESI) m/z = 349 [M+H]$^+$; HRMS (ESI): m/z calcd for C$_{20}$H$_{17}$N$_2$O$_4$: 349.1188; found: 349.1177 [M+H]$^+$.

4.9.2. (E)-Methyl 3-(4-(((5,8-dioxo-5,8-dihydroquinolin-7-yl)amino)methyl)phenyl) acrylate (7g)

Analytical data for **7g**: ^{1}H NMR (d_6-CD$_3$OD, 400 MHz): δ 8.82 (d, 1H, J = 4.0 Hz, Ar-H), 8.38 (d, 1H, J = 4.0 Hz, Ar-H), 7.67 (m, 1H, Ar-H), 7.66 (s, 1H, Ar-H), 7.58 (s, 1H, CH), 7.52 (d, 1H, J = 6.0 Hz, Ar-H), 7.38 (m, 2H, Ar-H), 6.51 (d, 1H, J = 16.0 Hz, CH), 5.68 (s, 1H, CH), 4.50 (s, 2H, CH$_2$), 3.73 (s, 3H, OCH$_3$). ^{13}C NMR (d_6-DMSO, 100 MHz): δ 181.1, 180.1, 167.0, 153.0, 149.6, 147.2, 144.8, 138.5, 134.6, 133.9, 130.5, 129.6, 128.8, 127.5, 118.3, 100.2, 52.0, 45.3. MS (ESI) m/z = 349 [M+H]$^+$; HRMS (ESI): m/z calcd for C$_{20}$H$_{17}$N$_2$O$_4$: 349.1188; found: 349.1177 [M+H]$^+$.

4.10. General procedure for synthesis of 6h, 7h

Compounds **6h** and **7h** were synthesized from quinoline-5,8-dione (**4**), (*E*)-methyl 3-(3-(aminomethyl)phenyl)acrylate (**10b**), according to the synthetic procedure for compounds **6a** and **7a** in yields of 35% and 22%, respectively.

4.10.1. (E)-Methyl 3-(3-(((5,8-dioxo-5,8-dihydroquinolin-6-yl)amino)methyl)phenyl)acrylate (6h)

Analytical data for **6h**: ^{1}H NMR (d_6-CD$_3$OD, 400 MHz): δ 8.80 (m, 1H, Ar-H), 8.37 (d, 1H, J = 8.0 Hz, Ar-H), 7.62 (m, 3H, Ar-H, CH), 7.53 (s, 1H, Ar-H), 7.33 (m, 2H, Ar-H), 6.48 (d, 1H, J = 16.0 Hz, CH), 5.74 (s, 1H, CH), 4.45 (s, 2H, CH$_2$), 3.68 (s, 3H, OCH$_3$). ^{13}C NMR (d_6-DMSO, 100 MHz): δ 181.9, 180.5, 167.0, 154.8, 148.9, 148.5, 144.8, 138.5, 134.5, 134.3, 129.6, 129.5, 128.0, 127.5, 127.4, 126.9, 118.4, 102.0, 51.9, 45.2. MS (ESI) m/z = 349 [M+H]$^+$; HRMS (ESI): m/z calcd for C$_{20}$H$_{17}$N$_2$O$_4$: 349.1188; found: 349.1179 [M+H]$^+$.

4.10.2. (E)-Methyl 3-(3-(((5,8-dioxo-5,8-dihydroquinolin-7-yl)amino)methyl)phenyl)acrylate (7h)

Analytical data for **7h**: ^{1}H NMR (d_6-CD$_3$OD, 400 MHz): δ 8.81 (m, 1H, Ar-H), 8.35 (d, 1H, J = 4.0 Hz, Ar-H), 7.62 (m, 3H, Ar-H, CH), 7.58 (s, 1H, Ar-H), 7.38 (m, 2H, Ar-H), 6.53 (d, 1H, J = 16.0 Hz, CH), 5.70 (s, 1H, CH), 4.53 (m, 2H, CH$_2$), 3.74 (s, 3H, OCH$_3$). ^{13}C NMR (d_6-DMSO, 100 MHz): δ 181.6, 169.5, 152.1, 149.4, 144.3, 134.8, 134.1, 131.6, 131.5, 129.0, 128.9, 128.5, 128.4, 126.9, 126.6, 117.7, 109.9, 99.8, 50.7, 45.3. MS (ESI) m/z = 349 [M+H]$^+$; HRMS (ESI): m/z calcd for C$_{20}$H$_{17}$N$_2$O$_4$: 349.1188; found: 349.1182 [M+H]$^+$.

4.11 Cell Culture

The multidrug resistant cancer cell line, KB-vin, was a generous gift from Dr. Kuo-Hsiung Lee (University of North Carolina, Chapel Hill, U.S.A) and maintained with vincristine. The drug sensitive cell line, HeLaS3, was purchased from Bioresource Collection and Research Center (Hsinchu, Taiwan). Human endometrial epithelial cells (EEC) were purchased from Shanghai Institute of Cell Biology (Shanghai, China). All cells were cultured in RPMI-1640 containing 10% FBS at 37°C in a humidified atmosphere of 5% CO$_2$.

4.12 Cell viability assay

The effects of test compounds on cell viability were evaluated by SRB and MTT assays. For the SRB assay, after 72 h treatment with serial concentrations of test compounds, 50% trichloroacetic acid (TCA) was added to fix cells for 30 min, and then the cells were washed with water and air-dried. Subsequently, cells were stained with 0.04% sulforhodamine B (SRB) for 30 min and washed with 1% acetic acid. The bound stain was solubilized in 10 mM Tris Base and the absorbance was measured by BioTek Synergy HT Multi-Mode Microplate Reader at 515 nm. For the MTT assay, 100 μL of different cancer cells were plated in a 96-well flat bottom tissue culture plate at a density of 10^4 cells/mL in DMEM medium containing 10% fetal bovine serum and allowed to adhere overnight at 37 °C in 5% CO$_2$. The cells were treated by adding 100 μL of different compounds at various concentrations into the respective well. The reagent DMSO (0.1%) was used as a negative control. The cell viability assay (MTT assay) was carried out at 72 h after drug treatment. The concentration that inhibited 50% of cellular growth (IC$_{50}$ value) was calculated by the following formula: Cell inhibition rate (%) = (1 − OD of treatment group/OD of control group) × 100%. To evaluate the NQO1 dependency, cell viabilities were evaluated by combination treatment of 10 μM dicoumarol or 40 μM N-acetylcysteine with test compounds. The cell viability was evaluated by SRB assay after 72 h treatment. The cytotoxic potency of test compounds on cancer cells was expressed as IC$_{50}$ values or by a histogram (The bars are the mean ± SD). All data were derived from three independent measurements.

4.13 NQO1 activity assay

The effects of test compounds (0.1 μM to 10 μM) on endogenous NQO1 activity were evaluated by the NQO1 activity assay kit (Abcam, Cambridge, MA, USA). Briefly, cell pellets were solubilized in 1X extraction buffer on ice for 20 minutes and then centrifuged at 18,000 × g for 20 minutes at 4°C. Supernatants were transferred to new tubes and protein concentrations were determined using the Bio-Rad protein assay method. Samples were diluted with supplemented buffer to 2X the working

concentration. Two wells were prepared for each sample (with and without inhibitor) in triplicate. The reaction buffer and the reaction buffer plus inhibitor were prepared according to the instruction of manufacturer. Absorbance was measured at 440 nm every 20 seconds for 5 minutes using the BioTek Synergy HT Multi-Mode Microplate Reader with shaking before reading.

4.14 NQO1 inhibitory kinetic assay

The inhibitory activity of recombinant human NQO1 was measured by the NQO1 activity assay kit (Abcam, Cambridge, MA, USA). The inhibitory kinetics of NQO1 were analyzed by Lineweaver-Burk plots and compared to no treatment control. To calculate the kinetic parameters of inhibition mechanism of NQO1, steady-state rates were obtained at various concentrations of test compounds and substrate.

4.15 Detection of ROS

The ROS-Glo H_2O_2 Assay (Promega®, Southampton, UK) was used to measure changes of ROS by directly detecting H_2O_2 in cells. The cells were plated in 96-well white tissue culture plates and then treated with test compounds (0.01 μM to 5 μM) for 24 h. The H_2O_2 substrate solution was added to each well and incubated for 6 h at 37 °C in a CO_2 incubator. After the incubation with H_2O_2 substrate, ROS-Glo Detection Solution was added to each well and incubated at room temperature for 20 min. The luminescence was detected by BioTek Synergy HT Multi-Mode Microplate Reader.

4.16 Mitochondrial membrane potential assay

The effects of test compounds on changes in the mitochondrial membrane potential (MMP) were detected by using the Mito-ID membrane potential cytotoxicity and detection kit (Enzo Life Sciences, Lausen, Switzerland) according to the manufacturer's instructions. Briefly, 2.5×10^5/mL cells were plated in 96-well black wall and clear bottom plates. The cells were treated with test compounds (0.01 μM to 5 μM), CCCP (positive control) and DMSO (vehicle control), respectively. After incubation for 24 hours at 37 °C, each well received 100 μL of the MITO-ID®MP Dye Loading Solution and was protected from light. Then, the plate was read with a BioTek Synergy HT Multi-Mode Microplate Reader using excitation at 490 nm and emission at 590 nm after incubation at 37 °C for 30 mins.

4.17 Flow cytometry assay of cell apoptosis

HeLaS3 cells were cultured overnight and incubated in triplicate with different concentrations of test compounds (0.2, 0.6, and 1.8 μM) or vehicle for 72 h. The cells were harvested and stained with FITC-Annexin V and PI at room temperature for 15 min. The percentage of apoptotic cells was determined by flow cytometry (Epics XL-MCL, Beckman Coulter, Indianapolis, USA) analysis. The FITC signal detector (FL1) and PI staining signal detector (FL3) were used to detect the cells with the flow cytometer (Ex = 488 nm; Em = 530 nm). Ten thousand cells were counted for three independent experiments. The data were analyzed using WinList 3D (version7.1) and the histogram was plotted using Excel 2010.

4.18 Western Blot Analysis

HeLaS3 cells at 1.5×10^5/mL were treated with different dosage of test compounds or vehicle control (0.1% of DMSO) in 2 mL DMEM medium supplemented with 10% FBS for 72 h. After being harvested and lyzed, the cell lysates (50 μg/lane) were separated by SDS-PAGE (12% gel) and transferred onto nitrocellulose membranes. After being blocked with 5% fat-free milk, the target proteins were probed with anti-Bax, anti-Bcl-2, anti-caspase 3, anti-cleaved-caspase 3, and anti-β-actin antibodies (Cell Signaling Technology, MA, USA), respectively. The bound antibodies were detected by HRP-conjugated second antibodies and visualized using the enhanced chemiluminescent reagent. The relative levels of each signaling event to control β-actin were determined by densimetric scanning.

Acknowledgement

References

[1] G. Waris, H. Ahsan, Reactive oxygen species: role in the development of cancer and various chronic conditions, J. Carcinog. 5 (2006) 14.

[2] W.S. Wu, The signaling mechanism of ROS in tumor progression, Cancer Metastasis Rev. 25 (2006) 695−705.

[3] Y. Lu, R. Zhang, S. Liu, Y. Zhao, J. Gao, L. Zhu, ZT-25, a new vacuolar H+-ATPase inhibitor, induces apoptosis and protective autophagy through ROS generation in HepG2 cells, Eur. J. Pharmacol. 771 (2016) 130-138.

[4] N.D. Amoedo, J.P. Valencia, M.F. Rodrigues, A. Galina, F.D. Rumjanek, How does the metabolism of tumour cells differ from that of normal cells, Biosci. Rep. 33 (2013) 865-873.

[5] J. Zhang, A. Yang, Y. Wu, W. Guan, B. Xiong, X. Peng, X. Wei, C. Chen, Z. Liu, Stachydrine ameliorates carbon tetrachloride-induced hepatic fibrosis by inhibiting inflammation, oxidative stress and regulating MMPs/TIMPs system in rats, Biomed. Pharmacother. 97 (2018) 1586-1594.

[6] C. Gorrini, I.S. Harris, T.W. Mak, Modulation of oxidative stress as an anticancer strategy, Nat. Rev. Drug Discovery. 12 (2013) 931−947.

[7] H. Ni, C. Xia, Y. Zhao, Synthesis, cytotoxicity and pro-apoptosis activity of isoquinoline quinones, Med. Chem. Res. 87 (2017) 88-94.

[8] J. Qin, M. Wu, S. Yu, X. Gao, J. Zhang, X. Dong, J. Ji, Y. Zhang, L. Zhou, Q. Zhang, F. Ding, Pyrroloquinoline quinone-conferred neuroprotection in rotenone models of Parkinson's disease, Toxicol. Lett. 238 (2015) 70-82.

[9] S. Danson, T.H. Ward, J. Butler, M. Ranson, Exploiting tumor hypoxia in cancer treatment,

Cancer Treat. Rev. 30 (2004) 437–449.

[10] A.M. Malkinson, D. Siegel, G.L. Forrest, A.F. Gazdar, H.K. Oie, D.C. Chan, P.A. Bunn, M. Mabry, D.J. Dykes, S.D. Harrison, D. Ross, Elevated DT-diaphorase activity and messenger RNA content in human non-small cell lung carcinoma: relationship to the response of lung tumor xenografts to mitomycin C, Cancer Res. 52 (1992) 4752–4757.

[11] M. Nakamura, T. Hayashi, J. Biochem, One- and two-electron reduction of quinones by rat liver subcellular fractions, J Biochens. 115 (1994) 1141–1147.

[12] S.L. Winski, Y. Koutalos, D.L. Bentley, D. Ross, Subcellular localization of NAD(P)H: quinone oxidoreductase 1 in human cancer, Cancer Res. 62 (2002) 1420–1424.

[13] H.J. Prochaska, C.L. Fernandes, Elevation of serum Phase II enzymes by anticarcinogenic enzyme inducers: markers for a cemoprotected state? Carcinogenesis. 14 (1993) 2441–2445.

[14] J.J. Schlager, B.J. Hoerl, J. Riebow, D.P. Scott, P. Gasdaska, R.E. Scott, G. Powis, Increased NAD(P)H:(quinone-acceptor)oxidoreductase activity is associated with density-dependent growth inhibition of normal but not transformed cells, Cancer Res. 53 (1993) 1338‒1342.

[15] E.H.G. da Cruz, M.A. Silvers, G.A.M. Jardim, J.M. Resende, B.C. Cavalcanti, I.S. Bomfim, C. Pessoa, C.A. de Simone, G.V. Botteselle, A.L. Braga, D.K. Nair, I.N.N. Namboothiri, D.A. Boothman, E.N. da Silva Júnior. Synthesis and antitumor activity of selenium-containing quinone-based triazoles possessing two redox centres, and their mechanistic insights. Eur. J. Med. Chem. 122 (2016) 1-16.

[16] C. Keyari, A. Kearns, N. Duncan, E. Eickholt, G. Abbott, H. Beall, P. Diaz, Synthesis of new quinolinequinone derivatives and preliminary exploration of their cytotoxic properties, J. Med. Chem. 56 (2013) 3806-3819.

[17] M. Hassani, W. Cai, D. Holley, J. Lineswala, B. Maharjan, G. Ebrahimian, H. Seradj, M. Stocksdale, F. Mohammadi, C. Marvin, J. Gerdes, H. Beall, M. Behforouz, Novel lavendamycin analogues as antitumor agents: synthesis, in vitro cytotoxicity, structure-metabolism, and computational molecular modeling studies with NAD(P)H: quinone Oxidoreductase 1, J. Med. Chem. 48 (2005) 7733-7749.

[18] C.K. Ryu, H.J. Jeong, S.K. Lee, H.J. You, K.U. Choi, J.Y. Shim, Y.H. Heo, C.O. Lee, Effects of 6-arylamino-5,8-quinolinediones and 6-chloro-7-arylamino-5,8-isoquinolinediones on NAD(P)H: quinone oxidoreductase (NQO1) activity and their cytotoxic potential, Arch. Pharm. Res. 24 (2001) 390-896.

[19] T. Fryatt, H.I. Pettersson, W.T. Gardipee, K.C. Bray, S.J. Green, A.M.Z. Slawin, H.D. Beall, C.J. Moody, Novel quinolinequinone antitumor agents: structure-metabolism studies with NAD(P)-H:quinone oxidoreductase (NQO1), Bioorg. Med. Chem. 12 (2004) 1667–1687.

[20] E. Swann, P. Barraja, A.M. Oberlander, W.T. Gardipee, A.R. Hudnott, H.D. Beall, C.J. Moody, Indolequinone antitumor agents: Correlation between quinone structure and rate of metabolism by recombinant human NAD(P)H:quinone oxidoreductase. Part 2, J. Med. Chem. 44 (2001) 3311–3319.

[21] M. Hassani, W. Cai, K.H. Koelsch, D.C. Holley, A.S. Rose, F. Olang, J.P. Lineswala, W.G. Holloway, J.M. Gerdes, M. Behforouz, H.D. Beall, Lavendamycin antitumor agents: Structure-based design, synthesis, and NAD(P)H:quinone oxidoreductase 1 (NQO1) model

validation with molecular docking and biological studies, J. Med. Chem. 51 (2008) 3104–3115.

[22] W. Cai, M. Hassani, R. Karki, E.D. Walter, K.H. Koelsch, H. Seradj, J.P. Lineswala, H. Mirzaei, J.S. York, F. Olang, M. Sedighi, J.S. Lucas, T.J. Eads, A.S. Rose, S. Charkhzarrin, N.G. Hermann, H.D. Beall, M. Behforouz, Synthesis, metabolism and in vitro cytotoxicity studies on novel lavendamycin antitumor agents, Bioorg. Med. Chem. 18 (2010) 1899–1909.

[23] J. Bian, X. Li, N. Wang, X. Wu, Q. You, X. Zhang, Discovery of quinone-directed antitumor agents selectively bioactivated by NQO1 over CPR with improved safety profile, Eur. J. Med. Chem. 129 (2017) 27-40.

[24] M. Kadela-Tomanek, M. Jastrzębska, B. Pawełczak, E. Bębenek, E. Chrobak, M. Latocha, M. Książek, J. Kusz, S. Boryczka, Alkynyloxy derivatives of 5,8-quinolinedione: Synthesis, in vitro cytotoxicity studies and computational molecular modeling with NAD(P)H:Quinone oxidoreductase 1, Eur. J. Med. Chem. 126 (2017) 969-982.

[25] H. Soedjak, J. Hajdu, J. Raffetto, R. Cano, B. Bales, L. Prasad, L. Kispert, The structure of streptonigrin semiquinone in solution, Biochim. Biophys. Acta. 1335 (1997) 73-90.

[26] R. Barret, M. Daudon, Oxidation of phenols to quinones by bis(trifluoroacetoxy)iodobenzene. Tetrahedron Lett. 31 (1990) 4871-4872.

[27] K.M. Aubart, C.H. Heathcock, A biomimetic approach to the discorhabdin alkaloids: total syntheses of discorhabdins C and E and dethiadiscorhabdin D, J. Org. Chem. 64 (1999) 16-22.

[28] S.E. Weinberg, N.S. Chandel, Targeting mitochondria metabolism for cancer therapy, Nat. Chem. Biol. 11 (2015) 9–15.

[29] M.L. Brown, M. Paige, J.A. Toretsky, A. Üren, G. Kosturko, G. Bulut, Novel Ezrin inhibitors and methods of making and using, PCT Int. Appl. (2012), WO2012064396 A2, 20120518.

Development of novel amino-5,8-quinolinedione derivatives as NAD(P)H: quinone-oxidoreductase-1 (NQO1) inhibitor with potent antiproliferative activities

Yong Ling[a,b,1], Qiu-Xing Yang[a,1], Yu-Ning Teng[b,c], Shi Chen[a], Wei-Jie Gao[a], Jing Guo[a], Pei-Ling Hsu[b], Yue Liu[a], Susan L. Morris-Natschke[b], Chin-Chuan Hung[c,*], Kuo-Hsiung Lee[b,d*]

[a]School of Pharmacy and Jiangsu Province Key Laboratory for Inflammation and Molecular Drug Target, Nantong University, Nantong 226001, PR China.

[b]Natural Products Research Laboratories, UNC Eshelman School of Pharmacy, University of North Carolina, Chapel Hill, North Carolina 27599, United States

[c]Department of Pharmacy, College of Pharmacy, China Medical University, Taichung 40402, Taiwan

[d]Chinese Medicine Research and Development Center, China Medical University and Hospital, Taichung 40402, Taiwan

Highlights

- Novel amino-5,8-quinolinedione derivatives were synthesized.
- All compounds showed significant antiproliferative potency in cancer cells.
- Four selected compounds exhibited potent NQO1 inhibitory effects.
- Active compounds increased ROS level and induced lethal mitochondrial dysfunction.
- The most potent compound triggered cell apoptosis by regulating apoptotic proteins.